New Journal of Physics
The open access journal for physics

Physics of ablative Rayleigh–Taylor and Landau–Darrieus instabilities

A R Piriz[1,3] **and N A Tahir**[2]

[1] ETSI Industriales, Universidad de Castilla-La Mancha and Instituto de Investigaciones Energéticas, E-13071 Ciudad Real, Spain
[2] GSI Helmholtzzentrum für Schwerionenforschung Darmstadt, D-64291 Darmstadt, Germany
E-mail: roberto.piriz@uclm.es

New Journal of Physics **15** (2013) 015013 (14pp)
Received 11 July 2012
Published 22 January 2013
Online at http://www.njp.org/
doi:10.1088/1367-2630/15/1/015013

Abstract. An analysis of the linear instability of Rayleigh–Taylor instability in ablation fronts and of Landau–Darrieus instability in laminar flames is performed by means of a physical model that allows for identifying the mechanisms that control the stability of both kinds of fronts. The stability behavior of each front is shown to be determined by the particular process of energy transport that drives it. The evolution of perturbations due to the instability is found to always lead to a change in the temperature gradients, but this effect gives place to a restoring force only if the driving mechanism is sensitive to this change, such as happens in ablation fronts driven by thermal conduction. In flame fronts, the driving mechanism is not sensitive to perturbations in the temperature gradient, but, instead, it is sensitive to the temperature perturbations. The latter give place to a force that induces the well known instability in the flame front even in the absence of a gravitational field. The force driving the flame instability as well as the force providing stabilization to an ablation front, are both obtained from the same theoretical framework. The stabilizing role of the lateral thermal conduction for short perturbation wavelengths is also analyzed.

[3] Author to whom any correspondence should be addressed.

Contents

1. Introduction

The ignition of an inertial confinement fusion (ICF) target is one of the most expected events that will surely boost the search for a new source of energy based on the thermonuclear fusion [1–4]. The Rayleigh–Taylor instability (RTI) at the ablation front is one of the most important factors determining the minimum energy required for ignition and high gain [5–8]. RTI also plays an important role in many problems of high energy density physics [9–14] as well as in astrophysics [15]. In a similar manner, the Landau–Darrieus instability (LDI), typically affecting premixed laminar flames, has been found to occur in the astrophysics framework in the explosions of supernovas [16, 17]. More recently, the LDI has been shown to also be present in an ablation front at the early stages of the ablation process when the critical surface is still close to the ablation front [19–25].

These two kinds of deflagration fronts present similarities that have been noticed since the earliest studies of RTI in ablation fronts [26–28]. The most recent works have taken advantage of these similarities by applying well established mathematical methods in combustion theory to the study of hydro-instabilities in the ablation front [21, 25]. However, similarities between ablation fronts and laminar flames have presented the apparently striking fact that, in the regime of relatively small perturbation wave numbers k ($kL_2 \ll 1$, where $k = 2\pi\lambda$, λ is the perturbation wavelength and L_2 is the width of the thermal conduction region or, in general, of the energy transport region) the types of stability behavior of both fronts are opposite. In fact, ablation fronts are stable for all the wave numbers above a certain cut-off value k_c that becomes smaller as the intensity of the gravitational field g reduces, so that when $g = 0$, it is stable for any perturbation wave number, such as predicted by theory [5–8] and observed in the experiments [22, 29, 30]. Contrastingly, in the same regime of small wave numbers, laminar flames are found to be unstable for all the values of k even when $g = 0$ [16]. Furthermore, for wave numbers such that $kL_2 \geqslant 1$, the lateral energy transport by thermal conduction makes laminar flames stable [17, 18].

Recently, some authors have claimed that the latter mechanism is also responsible for the stability of ablation fronts for $k \geqslant k_c$ [21, 31]. This is in contradiction with the most current physical interpretation based on the dynamic overpressure in the perturbation valleys (under-pressure in the perturbation peaks), caused by the changes of the mass ablation rate due to the steepening (flattening) of the perturbed temperature gradient [8, 22–25, 32].

Here, we present an analysis of the physics of the instability of both kinds of deflagration fronts in the linear regime in order to evidence that the mechanisms that act on them at different

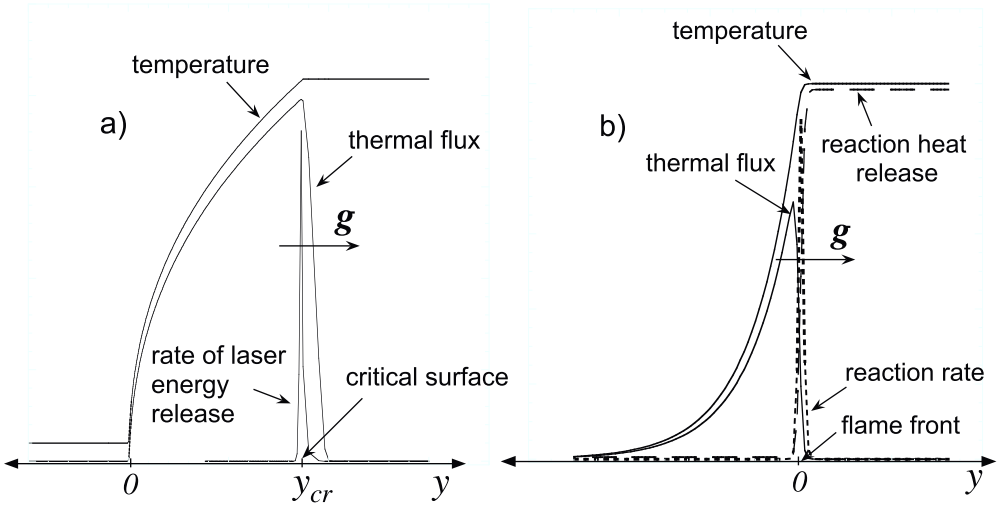

Figure 1. Schematic representation of the front structures for: (a) ablation front and (b) laminar flame.

ranges of perturbation wave numbers driving the instability or providing stabilization. For this purpose, rather than emphasizing the similarities between the fronts, we will discuss the main differences that lead to distinct stability behavior, especially in the regime of relatively short perturbation wavelengths, and provided that, in the case of an ablation front placed at $y = 0$, the critical surface location y_{cr} is relatively far from it ($ky_{cr} \gg 1$). The main differences between the structures of these fronts are schematically shown in figure 1 for the case in which the ablation front is driven by laser radiation. In the latter case, the laser beam deposits its energy at the critical surface ($y = y_{cr}$) and the energy is transported to the ablation surface by thermal conduction instead of being directly deposited on the front by the laser. That is, the ablation front is actually driven by thermal conduction. In the case of a flame front, it is instead driven by the chemical (or nuclear) energy released in the combustion process, while thermal conduction acts by transporting this energy away from the front. As a consequence, in spite of the fact that the temperature grows through the front in both the ablation and the flame cases, the thermal flux rate decreases behind a laminar flame (figure 1(b)) while it increases behind an ablation front (figure 1(a)).

Such differences determine that, behind the flame front, the flux of internal energy is balanced by the combustion energy release instead of being balanced by the thermal flux as happens behind the ablation front. In this work we will see that these differences are sufficient to explain the different stability performance of each kind of deflagration, and we will show that there are no reasons for assuming that the same stabilization mechanism must be present in any deflagration front when $kL_2 \ll 1$. In order to perform our stability analysis we will use the physical model for the instabilities evolution developed in [9–12, 32].

2. Analytic physical model

We consider the problem of a deflagration front of zero thickness placed at $y = \xi(x, t)$ and separating two ideal fluids of densities ρ_2 and ρ_1, respectively ($\rho_1 < \rho_2$). The fluids are in a uniform gravitational field with g pointing in the positive direction of the y-axis, which is taken

in the direction opposite to the density gradient (in the direction of the temperature gradient in figure 1).

We have shown in previous works that the stability analysis of the front can be performed by considering the balance of forces on the interface in order to describe the time evolution of the perturbations on it [9–12, 32]. According to such a physical model the equation of motion of the interface due to the instability is given by Newton's second law as follows:

$$\frac{\mathrm{d}}{\mathrm{d}t}\left[(m_1+m_2)\dot{\xi}\right]=\delta\Pi_{yy}^{(1)}n_y^{(1)}+\delta\Pi_{yy}^{(2)}n_y^{(2)}, \tag{1}$$

where $n_y^{(\nu)}$ is the vertical component of the unit vector $\mathbf{n}^{(\nu)}$ directed outward along the normal to the interface ($n_y^{(2)}=-n_y^{(1)}$) and $\delta\Pi_{yy}^{(\nu)}$ is the main vertical component of the perturbed momentum flux density tensor in the medium ν ($\nu=1,2$). For an ideal fluid the momentum flux density tensor reads [33]

$$\Pi_{ik}^{(\nu)}=p^{(\nu)}\delta_{ik}+\rho_\nu v_i^{(\nu)}u_k^{(\nu)}, \tag{2}$$

where $p^{(\nu)}$ and ρ_ν are, respectively, the pressure and density in the fluid, ν; $v_i^{(\nu)}$ are the fluid velocities in each medium relative to the interface and $u_i^{(\nu)}$ are the front or the fluid velocities relative to an inertial frame of reference. To zero order, in equilibrium, the front can be considered to propagate with constant velocity and we can take $u_i^{(\nu)}=v_i^{(\nu)}$. But when the front moves due to the instability, the perturbation growth is accelerated and therefore the differences between $u_i^{(\nu)}$ and $v_i^{(\nu)}$ must be taken into account. Besides, in equation (1) $\delta\Pi_{yy}^{(\nu)}n_y^{(\nu)}$ is the vertical force due to the fluid ν, provided we are in the linear regime for which $\delta\Pi_{xy}^{(\nu)}n_x^{(\nu)}\ll\delta\Pi_{yy}^{(\nu)}n_y^{(\nu)}$. In fact, in the linear regime it is $n_x^{(\nu)}\sim k\xi\ll 1$ and $|n_y^{(\nu)}|\approx 1$. Thus the right hand side of equation (1) represents the total vertical force acting on the interface due to the perturbations, and the left hand side represents the total momentum change, both per unitary area. In addition, in equation (1), m_ν are the masses (per unitary area) of each fluid that is involved in the motion caused by the instability. Since we are dealing with surface modes that decay exponentially from the interface with the characteristic length k^{-1}, we can write

$$m_\nu=\frac{\rho_\nu}{k}, \tag{3}$$

where, consistently, we will take ρ_ν as the density at $y=\pm\alpha k^{-1}$ for $\nu=1,2$, respectively:

$$\rho_1=\rho(\alpha k^{-1}),\qquad \rho_2=\rho(-\alpha k^{-1}), \tag{4}$$

where α is an unknown parameter of the order of unity that must be determined from comparison with self-consistent models like, for instance, those of [5–7]. Actually, this is just the condition referred to in the literature as the *closure condition* required for introducing the information regarding the front structure when a sharp boundary model (SBM) is used.

On the other hand, the perturbed momentum flux density tensor turns out to be as follows:

$$\delta\Pi_{yy}^{(\nu)}=\delta p^{(\nu)}+\dot{m}\delta u_\nu+\delta\dot{m}_\nu v_\nu, \tag{5}$$

where δu_ν is the perturbation in the velocity $u_y^{(\nu)}$, and the pressure perturbation $\delta p^{(\nu)}$ can be obtained as in [9–12] by considering that in equilibrium the pressure just on the interface is p_0 in both fluids. However, when it is displaced a small distance ξ from the equilibrium ($\xi>0$ for

$y > 0$) by a perturbation, the pressure in each fluid, just on the interface, increases (for $\xi > 0$) by the amount given by the Pascal hydrostatic law:

$$p^{(1)} = p_0 + \rho_1\, g\xi, \quad p^{(2)} = p_0 + \rho_2\, g\xi, \tag{6}$$

where $p_0 = \rho_2 gh$ and h is the thickness of the cold and dense fluid which is assumed here to satisfy the condition $kh \gg 1$. According to equation (6), the pressure perturbations $\delta p^{(\nu)}$ to be introduced into equation (5) are

$$\delta p^{(1)} = \rho_1\, g\xi, \quad \delta p^{(2)} = \rho_2\, g\xi. \tag{7}$$

Then, equation (1) can be written as follows:

$$2\dot{m}\dot{\xi} + \frac{\rho_1 + \rho_2}{k}\ddot{\xi} = (\rho_2 - \rho_1)g\xi - \dot{m}(\delta u_2 - \delta u_1) + \delta\dot{m}v_2 - \delta\dot{m}v_1. \tag{8}$$

In the previous equation, the first term on the left hand side is a damping force (proportional to $\dot{\xi}$) producing an effect similar to the viscosity in the evolution of RTI in Newtonian fluids [34, 35], and this effect is usually referred to in the literature as the *fire polishing* effect [8, 26]. The second term is, of course the momentum change due to the perturbation acceleration $\ddot{\xi}$. In addition, the first term of the right hand side is the buoyancy force that drives the RTI in any deflagration front. Notice that equation (8) has been written without any specification of the physics that define a particular kind of deflagration. However, although we need to add some extra physics in order to evaluate the last two terms on the right hand side of equation (8), we can still observe that the second term on the right hand side represents the effect of the convection, and that the last term includes the effect of the perturbation in the mass ablation rate. It may be worth mentioning that these two terms may, in principle, contribute in any manner, depending on the transport mechanism driving the front [32]. That is, they can introduce new destabilizing forces that, together with buoyancy, could accelerate the instability growth, or they can give rise to restoring forces that could eventually lead to the front stabilization.

In any case, as a general feature of ablation fronts and laminar flames, the interface is an isotherm and therefore the temperature at the interface remains invariant as it moves due to the instability [26]. It may be worth remarking that, strictly speaking, this is a boundary condition that defines the instantaneous position of the corrugated front. As a consequence, when the perturbation produces a local displacement of the interface from $y = 0$ to ξ, the perturbed temperature at $y = \xi$ is $\epsilon(\xi) = \epsilon_0(0)$. Actually, ϵ is the specific internal energy and it is used here as an equivalent to the temperature (the subindex '0' indicates unperturbed values). Then, the temperature perturbation is [8]

$$\delta\epsilon = \epsilon(\xi) - \epsilon_0(\xi) = -[\epsilon_0(\xi) - \epsilon_0(0)] = -\xi\frac{\mathrm{d}\epsilon}{\mathrm{d}y}. \tag{9}$$

Equation (9) is the corresponding boundary condition for the perturbations of the equilibrium boundary condition, setting that the temperature of the cold side of the front is fixed. It is interesting to note that it was actually the recognition of this boundary condition in [8] which made it possible to obtain correct results with the SBM for the RTI analysis, and not the lack of a *closure condition* related to the front structure, as was argued for a long time to explain the failure of the SBM. In fact, the latter is trivially given by equation (4) and it was not a real impediment for obtaining the correct growth rate in terms of an undefined density jump.

In order to evaluate the last two terms on the right hand side of equation (8) we need to specify the kind of front we are considering and the mechanisms of energy transport that drive

the corresponding deflagration. We will consider first the case of an ablation front driven by thermal diffusion. In the case that the thermal conduction is transporting the energy deposited by laser radiation at the critical surface $y = y_{cr}$, we will consider that $ky_{cr} \gg 1$.

2.1. Ablation fronts

We first evaluate the second term on the right hand side of equation (8) by specifying the perturbations δu_2 of the front velocity and δu_1 of the fluid behind the front as seen from an inertial system of reference. If we consider that the velocity of the fluid behind the front does not change due to the perturbations then a local reduction of the front velocity by an amount $\dot{\xi}$, that is $\delta u_2 = -\dot{\xi}$, will produce an increment of the fluid velocity behind the front by the same amount:

$$\delta u_2 = -\dot{\xi}, \quad \delta u_1 = +\dot{\xi}. \tag{10}$$

Thus, the term describing the convection effects becomes

$$\dot{m}(\delta u_2 - \delta u_1) = -2\dot{m}\dot{\xi}, \tag{11}$$

and it yields the other contribution, besides the fire polishing effect, to the damping term in the equation of motion of the interface. These two terms have an effect equivalent to the viscosity in RTI in Newtonian fluids [9, 10, 34, 35].

For the evaluation of the last term on the right hand side of equation (8) we must recall the energy conservation equation and specify the particular mechanism of energy transport that drives the ablation process. We will consider here the most typical case in which such a transport mechanism is thermal conduction with a thermal flux Q_T given by the Fourier law:

$$Q_T = -\kappa_D \frac{d\epsilon}{dy}, \quad \kappa_D = \chi \epsilon^n, \tag{12}$$

where χ is the coefficient of thermal conductivity and n is a number equal to $5/2$ for electronic thermal conduction but this is usually used to simulate other diffusive processes, such as thermal radiation, by assigning different values. With the previous assumption, the equilibrium profiles of the ablative corona in the region $y \ll y_{cr}$, where the isothermal Mach number is $M_1^2 = v_1^2/[(\gamma - 1)\epsilon] \ll 1$ (γ is the enthalpy coefficient), can be described by the following equations [5–8]:

$$Q_T \approx \gamma \dot{m}(\epsilon - \epsilon_\infty), \tag{13}$$

$$p \approx p_2 = \text{const.}, \tag{14}$$

$$\frac{\epsilon}{\epsilon_2} \approx \frac{v}{v_2} \approx \frac{\rho_2}{\rho}, \tag{15}$$

where ϵ_∞ is the specific internal energy for $y \to -\infty$, and ϵ_2 and v_2 are the values of these magnitudes taken at $y = -\alpha k^{-1}$. Here equations (12)–(15) serve a double purpose. Firstly, we can obtain the profiles to be used to evaluate the consistent values of the densities ρ_1 and ρ_2 as given by equation (4):

$$\frac{y}{L_2} = \int_1^\theta \frac{\theta^n}{\theta - 1} d\theta, \quad \theta = \frac{\epsilon}{\epsilon_2}, \quad L_2 = \frac{\chi \epsilon_2^n}{\gamma \dot{m}}. \tag{16}$$

Secondly, by taking into account that perturbations decay exponentially from the interface [$\delta\epsilon_1 \sim \exp(-ky)$], from equations (9) and (12) we obtain

$$\delta Q_{T1} = -\kappa_D k \delta\epsilon_1 = k\xi Q_{T1}. \tag{17}$$

On the other hand, when we move with the isotherm of the ablation front, the perturbation in the mass ablation rate $\delta\dot{m}_1$, for $y > 0$, turns out from equation (13):

$$\frac{\delta\dot{m}_1}{\dot{m}} = \frac{\delta Q_{T1}}{Q_{T1}} = k\xi. \tag{18}$$

In a similar manner, for $y < 0$ ($\delta\epsilon_2 \sim \exp(+ky)$), we get

$$\frac{\delta\dot{m}_2}{\dot{m}} = -k\xi. \tag{19}$$

Equations (18) and (19) yield the following expression for the last term on the right hand side of equation (8):

$$\delta\dot{m}_2 v_2 - \delta\dot{m}_1 v_1 = -k\xi\dot{m}(v_1 + v_2). \tag{20}$$

This term, proportional to the instantaneous amplitude ξ, is the restoring force (per unitary area) that opposes the buoyancy force due to gravity and leads to the total stabilization of the front for a sufficiently large wave number $k = k_c$ (the cut-off wave number). Following the analogy with RTI in Newtonian fluids, this term has an effect equivalent to surface tension.

Introducing equations (11) and (20) into equation (8), we obtain the equation of motion that leads to the well known asymptotic growth rate for the ablative RTI in the regime $kL_2 \ll 1$ [6–12, 32, 34, 35]:

$$\ddot{\xi} + \frac{4kv_2}{1+r_D}\dot{\xi} + kg\left(\frac{kv_2^2}{gr_D} - A_T\right)\xi = 0, \tag{21}$$

where

$$A_T = \frac{1-r_D}{1+r_D}, \quad r_D = \frac{\rho_1}{\rho_2}, \tag{22}$$

and r_D is calculated from equation (16). For the case of electronic thermal conduction it is $n = 5/2$ and we have that $\rho_2 \approx \rho(y \to -\infty)$. Thus, taking into account equation (4), the result is [8, 32, 34]

$$\frac{\alpha}{kL_2} \approx \frac{2}{5}\left(\frac{1}{r_D^{5/2}} - 1\right) + \frac{2}{3}\left(\frac{1}{r_D^{3/2}} - 1\right) + 2\left(\frac{1}{r_D^{1/2}} - 1\right). \tag{23}$$

It is worth remarking that equations (18) and (19) do not reflect any universal property of ablation fronts and they are only found for ablation fronts driven by a diffusive mechanism of energy transport similar to that given by equation (12). In fact, as shown in [32] and confirmed by two-dimensional numerical simulations [36, 37], the situation is different for ablation fronts driven by ion beams in which thermal conduction does not play a relevant role. In such a case $\delta\dot{m}_v/\dot{m} \ll k\xi$ and the main stabilization mechanism described by the restoring force of equation (20) is absent. Thus, the ablation front driven by ion beams is unstable, as it was already

known from early numerical simulations in the ion beam fusion framework [37]. The reason is clearly understood from the physical meaning of equations (9), (18) and (19). That is, when the isotherm of the front moves as a consequence of the instability, the cold material in the valleys enters a hotter region thus steepening the temperature gradient. Since the energy flux driving the ablation is transported by thermal conduction, it increases and then the mass ablation rate is also enhanced in the valleys, although its temperature has been reduced. As a consequence, a dynamic overpressure is created (equation (20)) that leads to the front stabilization. The same mechanism operates in the opposite manner in the peaks with the equivalent result ('peaks' and 'valleys' are defined in relation to the gravity orientation). In general terms this is called 'ablative stabilization', and it is certainly a rather misleading denomination since ablation by itself does not ensure the front stability [32]. In fact, if the energy flux driving the ablation is insensitive to the temperature gradient, as in the case of ablation driven by ion beams, no restoring force is generated and the resulting front is unstable for all the perturbation wave numbers with the only mitigation effect provided by the damping terms proportional to $\dot{\xi}$ in equation (21) [32, 37]. Actually, this effect should more appropriately be called *thermal conduction stabilization*.

In any case, the above analysis, as well as the comparison with the case of ion beam driven ablation, clearly shows the role of the steepening (flattening) of the temperature gradient at the valleys (peaks) as the main stabilizing mechanism acting on ablation fronts driven by thermal diffusion in the wave number range $L_2 \ll k^{-1} \ll y_{\mathrm{cr}}$. The dominance of this mechanism in ablation fronts seems to have been doubted by some authors on the basis of a comparison with the instability of laminar flames [21]. Therefore, in the next subsection we will consider the case of LDI in laminar flames to explore how the energy transport process that drives them leads to stability behavior different from that of ablation fronts driven by thermal conduction.

2.2. *Laminar flames*

As in the previous subsection, we start from equation (8) in order to obtain the evolution equation for the instability of a flame front and, as before, we have to evaluate the last two terms on the right hand side of that equation. For this, we need to know the perturbation δu_1 of the fluid behind the front, seen from an inertial reference frame when the front velocity decreases in a valley in such a manner that $\delta u_2 = -\dot{\xi}$. According to the well known *Landau–Darrieus condition* the perturbation in the fluid velocity behind the front is equal to the perturbation of the velocity of the flame front [16, 33]:

$$\delta u_2 = \delta u_1 = -\dot{\xi}. \tag{24}$$

This condition shows us the first difference from the ablation fronts since now the term describing the convection effect in equation (8) is

$$\dot{m}(\delta u_2 - \delta u_1) = 0, \tag{25}$$

and the only damping effect (the terms proportional to $\dot{\xi}$) comes from the *fire polishing* effect given by the first term on the left hand side of equation (8).

For evaluating the last term of equation (8) we can again consider that thermal conduction is given by equation (12). Momentum and mass conservation equations are still written as in equations (14) and (15), respectively but, instead, equation (13) represents the energy

conservation only for $y < 0$. However, in general, in the energy balance we have to include the heat release Q_R due to the combustion process taking place on the flame front ($kL_2 \ll 1$):

$$\frac{dQ_T}{dy} + \dot{q}_R = \frac{d(\gamma \dot{m} \epsilon)}{dy}, \tag{26}$$

where $\dot{q}_R = dQ_R/dy$ is the reaction rate. Then, for $y > 0$, we have

$$Q_R \approx \gamma \dot{m}(\epsilon_1 - \epsilon_\infty) \approx Q_T(0). \tag{27}$$

On the other hand, by following the Zeldovich arguments [16, 17] for calculating the flame velocity propagation, for $y \geqslant 0$ and in the conduction zone ($y \approx 0^+$), we have

$$Q_T + Q_R \approx \text{const.} \tag{28}$$

Therefore,

$$\delta Q_R \approx \delta Q_T = -k\xi Q_T(0) = -k\xi Q_R, \tag{29}$$

where we have considered the flame front as an isotherm and then we have proceeded as in equation (17) and used equation (9). Therefore, using equation (27) we get for $y > 0$:

$$\frac{\delta \dot{m}_1}{\dot{m}} = \frac{\delta Q_R}{Q_R} = -k\xi. \tag{30}$$

Compare this result with equation (18) for the case of an ablation front and notice that $\delta \dot{m}_1$ is of the same magnitude as before but now it is negative. Instead, ahead of the front, equations (9) and (12)–(15) are valid and we get the same result as for an ablation front:

$$\frac{\delta \dot{m}_2}{\dot{m}} = -k\xi. \tag{31}$$

Equations (30) and (31) allows us to calculate the last term of equation (8) to yield the following result:

$$\delta \dot{m}_2 v_2 - \delta \dot{m}_1 v_1 = k\xi \dot{m}(v_1 - v_2). \tag{32}$$

It is worth noting in the previous equation that now only the perturbation in mass ablation rate due to the thermal conduction ahead the front is able to generate a restoring force such as the one observed in ablation fronts. Instead, behind the flame front, the force that drives the LDI is created and overcomes the restoring effects created ahead of it. This LDI driving force is $k\xi \dot{m} v_1$ and it originates in the fact that the thermal flux rate $\dot{Q}_T = dQ_T/dy$ is negative behind the front. Thus, although in an ablation front the perturbation causes the enhancement of the temperature gradient (and of the thermal conduction flux), in the laminar flame the same effect leads to a reduction in the heat release Q_R which drives the front. As a consequence the mass flux $\dot{m}$ is reduced to ($\delta \dot{m}_1$). In the simplest terms, when the cold matter in the valleys enters a hotter region and cools it, the reaction rate decreases, the mass flux reduces and a dynamic *under-pressure* occurs at the valleys thus accelerating the front deformation. Of course, the same mechanism operates in the peaks in the opposite manner with the same result. We recall once again that, in the ablation front, stabilization only occurs when the front is driven by thermal conduction. In a laminar flame the front is driven by the energy release Q_R due to the combustion process and it is not drastically affected by changes in the temperature gradient. Therefore, the main stabilizing mechanism present in ablation fronts is absent in laminar flames. Furthermore, since

the flame is driven by a process different from the one driving ablation, a destabilizing force is created that make the flame unstable even in the absence of gravity ($g = 0$).

By introducing equations (25) and (32) into equation (8), it yields [16, 33]

$$\ddot{\xi} + \frac{2kv_2}{1+r_D}\dot{\xi} - A_T kg\left(\frac{kv_2^2}{gr_D} + 1\right)\xi = 0. \tag{33}$$

This equation describes the flame front instability due the combination of LD and RT instabilities for $kL_2 \ll 1$. For $g = 0$ we get the well known result for the LDI in laminar flames. In equation (33) the density jump $r_D = \rho(+\alpha k^{-1})/\rho(-\alpha k^{-1})$ is calculated from equations (12) and (13) as in the previous section (equation (16))

$$\frac{\alpha}{kL_2} = \int_{r_D/r_{D\infty}}^{1/r_{D\infty}} \frac{\theta^n}{\theta - 1}\mathrm{d}\theta, \quad r_{D\infty} = \frac{\epsilon_\infty}{\epsilon_1}, \tag{34}$$

where α is a parameter chosen to fit self-consistent models or numerical simulations. For the typical case of $n = 0$ considered in combustion theory, we have

$$r_D = r_{D\infty} + (1 - r_{D\infty})\mathrm{e}^{-\alpha/kL_2}. \tag{35}$$

Since we are in the regime $kL_2 \ll 1$, the result is $r_D \approx r_{D\infty}$, such as that usually taken in LDI in flame fronts.

3. Lateral thermal transport

Recently, some authors have argued on the basis of a comparison of ablation fronts with laminar flames that the dominant mechanism of stabilization on the former was lateral transport by thermal conduction [21]. Actually, we should expect that the lateral transport of mass, momentum and energy becomes relevant when the characteristic length of the conduction region is of the order of k^{-1}. In fact, we have seen in the previous section that in the regime $kL_2 \ll 1$ the flame fronts are unstable and the ablation fronts are stable for $k \geqslant k_c$ due to the restoring force arising from the self-regulation of the thermal conduction normal to the interface. It is out of the scope of this work to evaluate all the effects of the lateral transport of mass, momentum and energy when $kL_2 \sim 1$, because it would probably require us to also consider the momentum equation in the direction parallel to the interface, which has not been considered in our physical model. However, we can approximately extend the energy conservation equation to include the lateral thermal transport in a similar manner as in [8]. Let us start with the case of an ablation front.

We can recalculate the perturbation $\delta\dot{m}_1$ in the mass ablation rate behind the front by including the lateral transport of energy by thermal conduction δq_x in the following manner [8]:

$$\gamma\delta\dot{m}_1(\epsilon - \epsilon_\infty) \approx -k\kappa_D\delta\epsilon_1 + \int_{-k^{-1}}^{k^{-1}} \frac{\partial\delta q_x}{\partial x}\,\mathrm{d}y. \tag{36}$$

By considering that the perturbations are of the form $\delta\varphi \sim \mathrm{e}^{\mathrm{i}kx}$, we have

$$\frac{\partial\delta q_x}{\partial x} = \mathrm{i}k\delta q_x = -k^2\kappa_D\delta\epsilon. \tag{37}$$

Using equation (9) and performing the integral, yields

$$\frac{\delta \dot{m}_1}{\dot{m}} = k\xi \left(1 + \frac{kL_2}{n+1} \frac{1 - r_D^{n+1}}{r_D^n (1 - r_D)}\right), \tag{38}$$

where we have also used equations (12) and (13). Then, the restoring force given by the last term of equation (8) becomes

$$\delta \dot{m}_2 v_2 - \delta \dot{m}_1 v_1 = -k\xi \dot{m} (v_1 + v_2) (1 + a_A k L_2), \tag{39}$$

$$a_A = \frac{1 - r_D^{n+1}}{(n+1) r_D^n (1 - r_D^2)}. \tag{40}$$

That is, the restoring force is now enhanced by a factor $1 + a_A k L_2$ as a consequence of the lateral thermal conduction. In general, as shown by equation (23) for $n = 5/2$, r_D is a function of kL_2 and, in any case, we can see that $a_A k L_2 \to 5\alpha/7$ for $kL_2 \to 0$. Therefore, as we expected, the lateral transport becomes a relevant stabilizing mechanism in ablation fronts when $a_A k L_2 \sim 1$. We can appreciate better the meaning of this by calculating the cut-off wave number k_c above which the front is stable:

$$\frac{k_c v_2^2}{g} (1 + a_A k L_2) = \frac{(1 - r_D) r_D}{1 + r_D}, \tag{41}$$

where we can use the approximate expression given by equation (23) for calculating r_D. The result is shown in figure 2 where the dimensionless cut-off $k_c v_2^2/g$ is represented as a function of the Froude number $Fr_2 = v_2^2/gL_2$, and we have taken $\alpha = 0.25$ in equation (23) in order to agree with the self-consistent models and the numerical calculations (closure condition). Thus, the value given by equation (41) coincides with the numerical calculations by Kull [5] and corresponds to the curve labeled in figure 2 as 'with lateral transport'. For comparison, the curve labeled 'no lateral transport' shows the dimensionless cut-off wave number given by equation (21) where lateral thermal conduction is neglected (with $\alpha = 0.38$). We have also represented the curves for r_D and $a_A k L_2$. We see that lateral thermal conduction is not an operative stabilizing mechanism for $Fr_2 \geqslant 3$ ($a_A k L_2 \leqslant 0.2$) and that its effects become the same order as the effect of the normal thermal conduction when $Fr_2 < 10^{-2}$. That is, although lateral transport is a relevant effect for small Froude numbers, it never becomes dominant in the range of values of interest in inertial fusion, provided that $k_c y_{cr} \ll 1$. In the opposite case ($k_c y_{cr} \geqslant 1$), the critical surface remains close to the ablation surface and the physical picture changes to the one corresponding to a flame as discussed in [19]. From the corona profiles of section 2.1, it turns out

$$\frac{y_{cr}}{L_2} \approx \left(\frac{\rho_2}{\rho_{cr}}\right)^n, \tag{42}$$

where ρ_{cr} is the critical density where the laser beam energy is deposited. Then, the condition $k_c y_{cr} \ll 1$ reads

$$Fr_2 \gg \left(\frac{n}{2}\right)^{1/n} \left(\frac{\rho_{cr}}{\rho_2}\right)^{n-1}. \tag{43}$$

In most cases of interest in ICF, the right hand side of equation (43) is a very small number except at the early stages of the ablation process when the ablation front instability behaves as in a laminar flame [19] and it was also studied in [21–25].

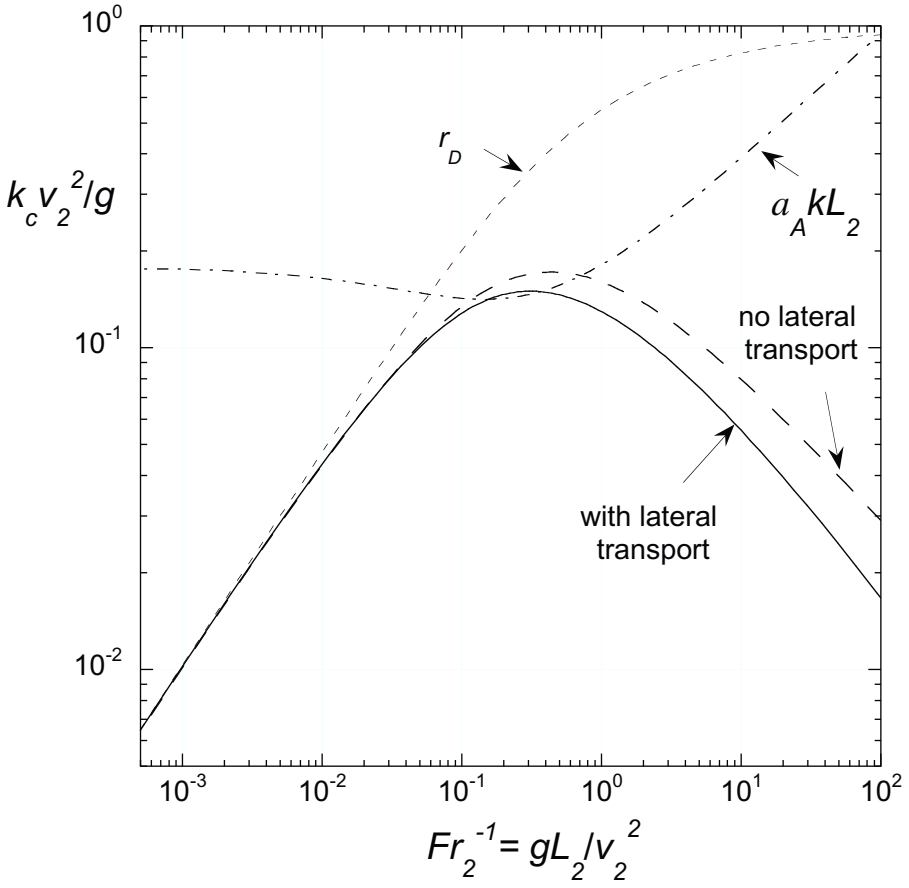

Figure 2. Dimensionless cut-off wave number as a function of the reciprocal of the Froude number Fr_2^{-1} for an ablation front driven by electronic thermal conduction ($n = 5/2$), with and without lateral thermal transport. The density jump r_D and the lateral transport term $a_A kL_2$ are also shown.

In a similar manner we can consider the lateral transport in a laminar flame:

$$\gamma \delta \dot{m}_2 (\epsilon_1 - \epsilon_\infty) \approx k \kappa_D \delta \epsilon_2 + \int_{-k^{-1}}^{k^{-1}} \frac{\partial \delta q_x}{\partial x} \mathrm{d}y, \tag{44}$$

$$\frac{\delta \dot{m}_2}{\dot{m}} = -k\xi \left(1 - \frac{kL_2}{n+1} \frac{1 - r_D^{n+1}}{r_D^n (1 - r_{D\infty})} \right), \tag{45}$$

and the last term of equation (8) is

$$\delta \dot{m}_2 v_2 - \delta \dot{m}_1 v_1 = k\xi \dot{m} (v_1 - v_2) (1 - a_F kL_2), \tag{46}$$

$$a_F = \frac{1 - r_D^{n+1}}{(n+1) r_D^n (1 - r_D)(1 - r_{D\infty})}. \tag{47}$$

This is not the exact result obtained with self-consistent models [21] but it captures the qualitative physical feature that, for $a_F kL_2 > 1$, equation (46) now represents a restoring force able to overcome the LD destabilization of the flame front. For the particular case of $n = 0$ it is $a_F \sim 1$. We see that in the case of laminar flames, lateral transport does not become operative

until $kL_2 \sim 1$, such as it happens in ablation fronts. But in flames it is the only stabilization mechanism, while ablation fronts exhibit stability due to normal thermal conduction for $k_c L_2 \leqslant 1$, provided that $k_c y_{cr} \gg 1$.

4. Concluding remarks

We have developed a physical model for the linear stability analysis of deflagration fronts such as ablation fronts and laminar flames in order to put in evidence that the apparently striking differences in the stability behavior of these two kinds of deflagrations are a consequence of the different processes of energy transport that drive both fronts.

We have shown that in ablation fronts the stabilizing mechanism arises mainly from the self-regulation of the mass ablation rate when the front is perturbed. Such a self-regulating process can be effective only when the deflagration front is driven by a diffusive process of energy deposition such as thermal conduction. Otherwise, if the corresponding process is not sensitive to the steepening (or flattening) of the temperature gradients, the stabilizing mechanism is not operative and the front turns out to be unstable, such as happens in ablation fronts driven by ion beams [32, 36, 37].

In the case of a laminar flame front, the process of energy transport driving the front is the energy release Q_R due to the combustion. This process is rather insensitive to the perturbations in the temperature gradient but, instead, it is affected by the temperature perturbations. Thus, in spite of the fact that the instability evolution induces perturbations in the temperature gradients, the mass flux $\dot{m}$ actually changes in response to the temperature perturbations. These effects lead to a reduction of $\dot{m}$ when the temperature is reduced, and it happens just when the temperature gradient is steepening. Therefore, the force driving the LDI is created as an under-pressure (over-pressure) in the perturbation valleys (peaks). This is the opposite mechanism to that operating in the ablation fronts.

In summary, depending on the particular mechanism of energy transport that drives the front, its perturbation can give origin to a restoring force, as in ablation driven by thermal conduction; to a null or very small force (neither restoring nor driving), as in ablation driven by ion beams; or to a driving force that eventually adds to the buoyancy force in the presence of a gravitational field, as in laminar flames.

Regarding RTI in ablation fronts, no new mechanism of stabilization exists beyond those already identified in [8] and, instead, the comparison with laminar flames sheds some light on the physical mechanism driving the LDI in laminar flames.

In the framework of ICF the picture that emerges from the previous results is consistent with the existing experimental [22, 28, 29] and simulation evidence [23, 38]. That is, LDI can dominate the perturbation evolution at the earliest stages of the laser–target interaction when the critical surface is still close to the ablation surface and the whole structure looks like a laminar flame (figure 1(b)). At these times the shock launched into the unablated part of the solid is still running inside it and $g \approx 0$ so that RTI is not yet operative while RMI is stabilized by the thermal conduction driving the ablation process. As the critical surface separates from the ablation front only the longest wavelengths will continue being LD unstable ($ky_{cr} < 1$). Then, when the target becomes accelerated and RTI is activated, it will immediately dominate the front instability for all the other wavelengths while LDI will be active for longer and longer wavelengths as both surfaces separate one from the other. In conclusion, LDI in an ablation front can be expected to be detected only at the earliest times of the interaction.

Acknowledgments

This work has been partially supported by the Ministerio de Economía y Competitividad of Spain (ENE2009-09276) and by the BMBF of Germany.

References

[1] Lindl J 1995 *Phys. Plasmas* **2** 3933
[2] Tahir N A and Long K A 1982 *Phys. Lett.* A **90** 242
[3] Long K A and Tahir N A 1986 *Nucl. Fusion* **26** 555
[4] Piriz A R 1988 *Phys. Fluids* **31** 658
[5] Kull H J 1989 *Phys. Fluids* B **1** 170
[6] Betti R, Goncharov V N, McCrory R and Verdon C P 1995 *Phys. Plasmas* **2** 3844
[7] Goncharov V N, Betti R, McCrory R, Sorotokin P and Verdon C P 1996 *Phys. Plasmas* **3** 1402
[8] Piriz A R, Sanz J and Ibañez L F 1997 *Phys. Plasmas* **4** 1117
[9] Piriz A R, Lopez Cela J J, Cortazar O D, Tahir N A and Hoffmann D H H 2005 *Phys. Rev.* E **72** 056313
[10] Piriz A R, Cortazar O D, Lopez Cela J J and Tahir N A 2006 *Am. J. Phys.* **74** 1095
[11] Piriz A R, Lopez Cela J J and Tahir N A 2009 *J. Appl. Phys.* **105** 116101
[12] Piriz A R, Lopez Cela J J and Tahir N A 2009 *Phys. Rev.* E **80** 046305
[13] Lopez Cela J J, Piriz A R, Serna Moreno M C and Tahir N A 2006 *Laser Part. Beams* **24** 427
[14] Tahir N A *et al* 2006 *Nucl. Instrum. Methods Phys. Res.* B **245** 85
[15] Remington B A, Drake R P and Ryutov D D 2006 *Rev. Mod. Phys.* **78** 755
[16] Zeldovich Ya B, Barenblatt G I, Librovich V B and Makhviladze G M 1985 *The Mathematical Theory of Combustion and Explosions* (New York: Consultant Bureau)
[17] Bychkov V V and Liberman M A 2000 *Phys. Rep.* **325** 115
[18] Pelce P and Clavin P 1982 *J. Fluid Mech.* **124** 219
[19] Piriz A R and Portugues R F 2003 *Phys. Plasmas* **10** 2449
[20] Piriz A R and Portugues R F 2003 *Plasma Phys. Control. Fusion* **46** 935
[21] Clavin P and Masse L 2004 *Phys. Plasmas* **11** 690
[22] Gotchev O V, Goncharov V N, Knauer J P, Boehly T R, Collins T J B, Epstein R, Jaanimagi P A and Meyerhofer D D 1997 *Phys. Rev. Lett.* **96** 115005
[23] Goncharov V N *et al* 2006 *Phys. Plasmas* **13** 012702
[24] Keskim M J, Velikovich A L and Schmitt A 2006 *Phys. Plasmas* **13** 122703
[25] Bychkov V, Modestov M and Marklund M 2008 *Phys. Plasmas* **15** 032702
[26] Bodner 1974 *Phys. Rev. Lett.* **33** 761
[27] Baker L 1978 *Phys. Fluids* **21** 295
[28] Baker L 1983 *Phys. Fluids* **26** 627
[29] Aglitskiy Y, Velikovich A L, Karasik M, Serlin V, Pawley C J, Schmitt A J, Obenschain S P, Mostovych A N, Gardner J H and Metzler N 2001 *Phys. Rev. Lett.* **87** 265001
[30] Aglitskiy Y *et al* 2009 *Phys. Rev. Lett.* **103** 085002
[31] Masse L 2007 *Phys. Rev. Lett.* **98** 245001
[32] Piriz S A, Piriz A R and Tahir N A 2009 *Phys. Plasmas* **16** 082706
[33] Landau L D and Lifshits E M 1987 *Fluid Mechanics* 2nd edn (Oxford: Pergamon)
[34] Piriz A R, DiLucchio L and Rodriguez Prieto G 2011 *Phys. Plasmas* **18** 012702
[35] Piriz A R, Piriz S A and Tahir N A 2011 *Phys. Plasmas* **18** 092705
[36] Perkins L J 2009 private communication
[37] Caruso A, Pais A and Parodi A 1992 *Laser Part. Beams* **10** 447
[38] Marocchino A, Atzeni S and Schiavi A 2010 *Phys. Plasmas* **17** 112703